# Diminished A-type potassium current and altered firing properties in presympathetic PVN neurones in renovascular hypertensive rats

Patrick M. Sonner, Jessica A. Filosa and Javier E. Stern

*Department of Psychiatry, University of Cincinnati, Cincinnati, OH, USA*

**Accumulating evidence supports a contribution of the hypothalamic paraventricular nucleus (PVN) to sympathoexcitation and elevated blood pressure in renovascular hypertension. However, the underlying mechanisms resulting in altered neuronal function in hypertensive rats remain largely unknown. Here, we aimed to address whether the transient outward potassium current ($I_A$) in identified rostral ventrolateral medulla (RVLM)-projecting PVN neurones is altered in hypertensive rats, and whether such changes affected single and repetitive action potential properties and associated changes in intracellular $Ca^{2+}$ levels. Patch-clamp recordings obtained from PVN-RVLM neurons showed a reduction in $I_A$ current magnitude and single channel conductance, and an enhanced steady-state current inactivation in hypertensive rats. Morphometric reconstructions of intracellularly labelled PVN-RVLM neurons showed a diminished dendritic surface area in hypertensive rats. Consistent with a diminished $I_A$ availability, action potentials in PVN-RVLM neurons in hypertensive rats were broader, decayed more slowly, and were less sensitive to the $K^+$ channel blocker 4-aminopyridine. Simultaneous patch clamp recordings and confocal $Ca^{2+}$ imaging demonstrated enhanced action potential-evoked intracellular $Ca^{2+}$ transients in hypertensive rats. Finally, spike broadening during repetitive firing discharge was enhanced in PVN-RVLM neurons from hypertensive rats. Altogether, our results indicate that diminished $I_A$ availability constitutes a contributing mechanism underlying aberrant central neuronal function in renovascular hypertension.**

(Resubmitted 29 October 2007; accepted after revision 24 January 2008; first published online 31 January 2008)
**Corresponding author** J. Stern: Department of Psychiatry, University of Cincinnati, Genome Research Institute, 2170 E. Galbraith Rd, Cincinnati, OH 45237, USA. Email: javier.stern@psychiatry.uc.edu

Elevated sympathetic outflow is known to contribute to the development and/or maintenance of hypertension, and is commonly observed in various forms of hypertensive disorders (Judy *et al.* 1976; Esler & Kaye, 1998; Guyenet, 2006), including those with a renovascular origin (Katholi *et al.* 1982; Oparil *et al.* 1987; Bergamaschi *et al.* 1995). While the initial phase of renovascular hypertension is primarily due to overactivation of the renin–angiontensin system (RAS), maintenance of high blood pressure at more established, chronic stages of the disease involves activation of neurogenic pressor mechanisms, including sustained sympathoexcitation (Martinez-Maldonado, 1991; Bergamaschi *et al.* 1995; Fink, 1997). While the precise pathophysiological mechanisms underlying sympathoexcitation in hypertensive individuals in general, and in renovascular hypertension in particular, remain largely unknown, accumulating evidence supports altered central control of autonomic function (Fink, 1997; Guyenet, 2006).

A growing body of evidence implicates the rostral ventrolateral medulla (RVLM) and the hypothalamic paraventricular nucleus (PVN), two key CNS presympathetic regions, as major underlying neuronal substrates in renovascular hypertension. An increased expression of FOS immunoreactivity in the RVLM was recently demonstrated in the two-kidney, one-clip Goldblatt renovascular model of hypertension (Jung *et al.* 2004). In addition, an enhanced excitatory glutamatergic activity within the RVLM was shown to contribute to elevated blood pressure in this model (Bergamaschi *et al.* 1995), an effect shown to be dependent on endogenous angiotensin II (AngII) (Carvalho *et al.* 2003).

A likely source contributing to enhanced glutamatergic activity in the RVLM of hypertensive rats is the PVN, an important homeostatic brain centre known to play a major role in the control of sympathetic outflow and regulation of blood pressure (Swanson & Sawchenko, 1983; Coote *et al.* 1998; Dampney *et al.* 2005). A major pathway by

© 2008 The Authors. Journal compilation © 2008 The Physiological Society DOI: 10.1113/jphysiol.2007.147413

which the PVN influences sympathetic activity involves a direct descending input to the RVLM (Ciriello *et al.* 1985; Dampney *et al.* 1987; Coote *et al.* 1998; Yang & Coote, 1998; Tagawa & Dampney, 1999; Kubo *et al.* 2000; Hardy, 2001; Allen, 2002), activation of which results in increased vasomotor RVLM neuronal activity (Yang *et al.* 2001). The PVN-RVLM pathway is largely composed of glutamatergic terminals (Stocker *et al.* 2006), and its over-activation contributes to sympathoexcitation and increased blood pressure in the spontaneously hypertensive rat (Allen, 2002). A role for the PVN in renovascular hypertension is also supported by studies showing that its electrolytic or chemical lesion inhibited the development and maintenance of renovascular hypertension (Earle *et al.* 1992; Earle & Pittman, 1995). In addition, an increased expression of FOS immunoreactivity was reported in the PVN of renovascular hypertensive rats (Jung *et al.* 2004), supporting an increased activation of PVN neurons, in renovascular hypertension. Thus, similarly to what is observed in other experimental models of hypertension (Nakata *et al.* 1989; Herzig *et al.* 1991; Lebrun *et al.* 1996; Allen, 2002; Davern & Head, 2007), activation of the PVN, in part through projections to the RVLM, contributes to sympathoexcitation and increased blood pressure in renovascular hypertension.

While an increased excitability of presympathetic PVN neurones was recently demonstrated in the spontaneously hypertensive rat (Li & Pan, 2006), the precise underlying cellular mechanisms remain unknown. Similar to other CNS neuronal populations, presympathetic PVN neuronal excitability and firing activity are fine-tuned by the combined actions of both intrinsic properties and synaptic inputs (Li *et al.* 2003; Cato & Toney, 2005; Li & Pan, 2005; 2007; Stocker *et al.* 2006; Sonner & Stern, 2007). While alterations in various PVN neurotransmitter systems (e.g. ANGII, GABA, nitric oxide, glutamate) have been reported in the PVN of hypertensive rats (Gutkind *et al.* 1988; Czyzewska-Szafran *et al.* 1989; DiCarlo *et al.* 2002; Jung *et al.* 2004; Li & Pan, 2006, 2007), including renal-dependent models (Petty & Reid, 1977; Martin & Haywood, 1998; Haywood *et al.* 2001; Jung *et al.* 2004), the potential contribution of altered intrinsic membrane properties to PVN neuronal hyperactivity during renovascular hypertension has not been thoroughly investigated.

In a recent study (Sonner & Stern, 2007), we showed that the voltage-dependent subthreshold A-type $K^+$ current ($I_A$) is a key intrinsic conductance regulating neuronal excitability in PVN-RVLM projecting neurones. We therefore investigated in this study whether changes in the biophysical properties of $I_A$ occurred in PVN-RVLM neurons in renovascular hypertensive rats, and whether they contributed to altered PVN neuronal excitability in this experimental hypertensive model. To this end we obtained electrophysiological and $Ca^{2+}$ imaging recordings from PVN-RVLM neurones in the Goldblatt two-kidney one-clip (2K1C) renovascular model of hypertension.

## Methods

Male Wistar rats ($n = 80$, 120–140 g) were purchased from Harlan laboratories (Indianapolis, IN, USA), and housed in a 12 h : 12 h light–dark cycle with access to food and water *ad libitum*. All procedures were carried out in agreement with the University of Cincinnati Animal Care and Use Committee's guidelines, and in compliance with NIH guidelines.

### Renovascular surgery

Rats weighing between 150 and 180 g (approximately 5–6 weeks old) were used to induce the renovascular 2K1C Goldblatt hypertension model, a well characterized and widely used model (Martinez-Maldonado, 1991; Bergamaschi *et al.* 1995). Rats were anaesthetized with isoflurane (3%) throughout the surgery. Following an abdominal incision, the left kidney was exposed, and a 0.2 mm clip was placed over the left renal artery, partially occluding it (Carvalho *et al.* 2003). Sham rats were subjected to the same surgical procedure, although the artery was not occluded. Post-operative care included proper management of associated pain (buprenorphine, 0.25 mg $kg^{-1}$, subcutaneous, as needed). Blood pressure was measured at the beginning of the sixth week post-surgery, using a tail-cuff method. All rats were used for experiments during the sixth–seventh week postsurgery.

### Retrograde labelling of preautonomic PVN neurones

Preautonomic RVLM-projecting PVN neurones were identified by injecting rhodamine beads unilaterally into the brainstem region containing the RVLM as previously described (Stern, 2001; Li *et al.* 2003) ($n = 69$ rats). Rats were anaesthetized (ketamine–xylazine mixture, 90 and 50 mg $kg^{-1}$, respectively, I.P.) and a stereotaxic apparatus was used to pressure inject 200 nl of rhodamine-labelled microspheres (Lumaflor, Naples, FL, USA) into the RVLM (starting from Bregma: 12 mm caudal along the lamina, 2 mm medial lateral, and 8 mm ventral). In general, RVLM injection sites were contained within the caudal pole of the facial nucleus to ~1 mm more caudal, and were ventrally located with respect to the nucleus ambiguous. In a subset of experiments ($n = 11$ rats), injections were also performed in the area of the dorsal vagal complex (DVC) (at the level of the obex: 1 mm lateral to the midline and 0.8 mm below the dorsal surface) to label DVC-projecting PVN neurons (Stern, 2001) as a control neuronal population. The location of the tracer was

© 2008 The Authors. Journal compilation © 2008 The Physiological Society

verified histologically (Stern, 2001; Li *et al.* 2003). As previously reported, retrogradely labelled neurones were found in the ventromedial (VM), dorsal cap (DC) and posterior (PaPo) PVN subnuclei (Armstrong *et al.* 1980; Swanson & Kuypers, 1980; Stern, 2001; Sonner & Stern, 2007). In some cases as indicated below, the subnucleus location of recorded, intracellularly filled neurones was determined.

### Hypothalamic slices

Two to three days after the retrograde injection, rats were anaesthetized with nembutal (50 mg $kg^{-1}$, I.P.), and perfused through the heart with a cold sucrose solution (containing, mM: 200 sucrose, 2.5 KCl, 3 $MgSO_4$, 26 $NaHCO_3$, 1.25 $NaH_2PO_4$, 20 D-glucose, 0.4 ascorbic acid, 1 $CaCl_2$ and 2 pyruvic acid (290–310 mosmol $l^{-1}$). Rats were then quickly decapitated, brains dissected out, and coronal slices cut (300 $\mu$m thick) using a vibroslicer (D.S.K. Microslicer, Ted Pella, Redding, CA, USA). An oxygenated ice cold artificial cerebrospinal fluid (ACSF) was used during slicing (containing, mM: 119 NaCl, 2.5 KCl, 1 $MgSO_4$, 26 $NaHCO_3$, 1.25 $NaH_2PO_4$, 20 D-glucose, 0.4 ascorbic acid, 2 $CaCl_2$ and 2 pyruvic acid; pH 7.4; 290–310 mosmol $l^{-1}$). Slices were placed in a holding chamber containing ACSF and kept at room temperature until used (see Stern, 2001 for details).

### Electrophysiology and data analysis

Slices were placed in a recording chamber, maintained at room temperature (~22–24°C), and bathed with solutions (~3.0 ml $min^{-1}$) that were continuously bubbled with 95% $O_2$–5% $CO_2$. Patch pipettes (4–8 MΩ) were pulled from thin-wall (1.5 mm outer diameter, 1.17 mm inner diameter) borosilicate glass (GC150T-7.5, Clark Electromedical Instruments, Reading, UK) on a horizontal electrode puller (P-97, Sutter Instrument Co., Novato, CA, USA). The internal solution contained (mM): 140 potassium gluconate, 0.2 EGTA, 10 Hepes, 10 KCl, 0.9 $MgCl_2$, 4 MgATP, 0.3 NaGTP and 20 phosphocreatine ($Na^+$); pH 7.2–7.3. A combination of fluorescence illumination and infrared differential interference contrast (IR-DIC) videomicroscopy was used to visualize fluorescently labelled preautonomic PVN neurones for whole-cell recordings. Recordings were obtained with a Multiclamp 700A amplifier (Axon Instruments, Union City, CA, USA). The voltage output was digitized at 16-bit resolution, 10 kHz (Digidata 1320A, Axon Instruments), and saved on a computer to be analysed offline. Data were discarded if the series resistance (13.15 ± 0.27 MΩ, $n = 168$) was not stable for the duration of the recording.

**Voltage-clamp recordings.** For voltage-clamp recordings, slices were bathed in an ACSF with nominal $Ca^{2+}$ (0 mM) (containing, mM: 102 NaCl, 2.5 KCl, 3 $MgSO_4$, 26 $NaHCO_3$, 1.25 $NaH_2PO4$, 20 D-glucose, 0.4 ascorbic acid, 2 pyruvic acid, 3 EGTA, 200 $\mu$M $CdCl_2$, 30 TEA and 0.5 $\mu$M TTX; pH 7.4; 290–310 mosmol $l^{-1}$). Series resistance was electronically compensated for at least 60% throughout the recordings. The voltage error of the half-activation and half-inactivation potentials due to uncompensated series resistance was 1.77 ± 0.12 mV and 1.31 ± 0.07 mV, respectively. All protocols were run with an output gain of 2 and a Bessel filter of 2 kHz, and were leak subtracted ($P/4$). The quality of the space clamp was assessed as previously described (Luther & Tasker, 2000; Sonner & Stern, 2007).

**Current-clamp recordings.** For current-clamp recordings, the ACSF contained (mM): 119 NaCl, 2.5 KCl, 1 $MgSO_4$, 26 $NaHCO_3$, 1.25 $NaH_2PO_4$, 20 D-glucose, 0.4 ascorbic acid, 2 $CaCl_2$, 2 pyruvic acid, 2 kynurenic acid, 0.3 picrotoxin; pH 7.4; 290–310 mosmol $l^{-1}$. All protocols run used an output gain of 10 and a Bessel filter of 10 kHz.

### Voltage dependence of activation of $I_A$

$I_A$ was isolated using a combination of digital and pharmacological methods. Calcium channels were blocked using a 0 $Ca^{2+}$ ACSF containing EGTA and $CdCl_2$, while $Na^+$ channels and delayed rectifier $K^+$ channels ($IK_{DR}$) were inhibited with TTX and TEA, respectively (see above). Two separate protocols were run in order to remove remaining TEA insensitive $IK_{DR}$ and further isolate $I_A$. The first utilized a hyperpolarized conditioning pulse (−90 mV), which removed inactivation from $I_A$. This pulse was followed by depolarizing command pulses (from −70 to +25 mV, 5 mV increments), which resulted in the activation of both $I_A$ and $IK_{DR}$. A second protocol, activating only $IK_{DR}$, was then run, in which a more depolarized (−40 mV) conditioning pulse was used to completely inactivate $I_A$. Currents recorded from these two protocols were then digitally subtracted offline using Clampfit 9.2 (Axon Instruments). The normalized $I_A$ peak amplitude was plotted as a function of the conditioning step potentials, and fitted with a Boltzmann function, to determine the half-activation potential. $I_A$ activation threshold was defined as the membrane potential at which a transient current ≥ 10 pA was detected. The current density was determined by dividing the current amplitude at each command potential by the cell capacitance, obtained by integrating the area under the transient capacitive phase of a 5 mV depolarizing step pulse, in voltage clamp mode. The rate of activation of $I_A$ was obtained by measuring the 10–90% rise time from the baseline to the peak of the current.

© 2008 The Authors. Journal compilation © 2008 The Physiological Society

### Voltage dependence of inactivation of $I_A$

In order to determine the voltage dependence of inactivation, a range of conditioning pulses (−120 to −35 mV, 50 ms) were utilized, to remove varying degrees of inactivation from $I_A$, followed by a command pulse to −10 mV to activate $I_A$. The normalized $I_A$ peak amplitude was plotted as a function of the conditioning step potentials, and fitted with a Boltzmann function to determine the half-inactivation potential. The inactivation $\tau$ of $I_A$ was determined by fitting a single exponential function to the decay phase of the current activated at −10 mV following a conditioning step to −90 mV.

### Kinetics of recovery from inactivation

The kinetics of recovery from inactivation were determined by applying a hyperpolarizing conditioning pulse (−100 mV) of increasing duration (Δ10 ms), followed by a command pulse to −10 mV. The normalized peak amplitude was plotted against the conditioning pulse duration. A single exponential function was fit to the plot and the time constant ($\tau$) of recovery from inactivation was then calculated.

### Non-stationary fluctuation analysis of $I_A$

For these studies, we followed procedures originally described by Sigworth (1980, 1981) and subsequently used by others (Robinson *et al.* 1991; Traynelis *et al.* 1993; De Koninck & Mody, 1994; Alvarez *et al.* 2002). Traces of $I_A$ ($n = 100$–130 traces) evoked with a command pulse to +40 mV were obtained and analysed with Mini Analysis software (Synaptosoft, Fort Lee, NJ, USA). The mean evoked current was scaled to individual $I_A$ waveforms. The difference between the scaled mean and the single current resulted in difference currents with a variance that was higher than background levels. The variance of the individual $I_A$ current around the scaled average was then computed and variance–amplitude relationships were plotted and fitted with a parabolic function. Values of unitary current, open probability and number of channels were calculated by Mini Analysis algorithms.

### Single and repetitive $Na^+$ action potential firing

To elicit individual action potentials, current was injected to maintain $V_m$ at ∼ −80 or ∼ −50 mV and subjected to brief depolarizing pulses (5 ms; 0.5–1.0 nA). At least 10 sweeps of evoked action potentials were averaged, and the mean action potential half-width and 90–10% decay time were analysed and compared before and after addition of the A-type $K^+$ channel blocker 4-AP, using algorithms provided by Mini Analysis software. Spontaneous firing activity was recorded in continuous mode. The mean firing frequency, from a period of 1–3 min, was calculated using Mini Analysis software. All action potentials within that period were averaged into a single spike waveform, and the mean action potential waveform was calculated and compared as above. To study spike broadening during repetitive firing, current was injected in order to maintain $V_m$ at ∼ −90 mV and depolarizing pulses (110–130 pA, 180 ms) were used to evoke firing discharge. The half-widths of the evoked action potentials were calculated. The degree of spike broadening was quantified as the ratio of the half-width of the third spike to that of the first spike (Shao *et al.* 1999; Stern, 2001). When needed, 4-AP was bath applied using a peristaltic pump (Gilson, Middleton, WI, USA; flow ∼2 ml $min^{-1}$) for a period of 5 min before recording its effects.

### Confocal calcium imaging

Dye-loading into identified retrogradely labelled PVN-RVLM neurones was achieved by addition of fluo-5F pentapotassium salt (100 μM; Invitrogen, Carlsbad, CA, USA) into the internal pipette solution. Once the whole-cell configuration was established, the dye was allowed to dialyse into the cell for at least 20 min before the initiation of the recordings. Calcium imaging was conducted using the Yokogawa real time live cell laser confocal system (CSU-10) combined with a highly sensitive EMCCD camera (iXon + 885, Andor Technology, South Windsor, CT, USA). Fluorescence images were obtained using diode-pumped solid-state laser (Melles Griot, Carlsbad, CA, USA), and fluorescence emission was collected at > 495 nm. Images were acquired at a rate of 40–50 Hz. The fractional fluorescence ($F/F_0$) was determined by dividing the fluorescence intensity ($F$) within a region of interest (ROI; 6 × 6 pixels, ∼4.8 × 4.8 μm) by a baseline fluorescence value ($F_0$) determined from 30 images before single action potentials were evoked (a period showing no change in intracellular calcium levels) (Filosa *et al.* 2004). The ROI was positioned within the cell soma, and care was taken to avoid the cell nucleus. Between 8 and 10 traces of calcium transients were averaged in order to increase the signal to noise ratio. Data were analysed using Andor IQ software (Andor, South Windsor, CT, USA).

### Neuronal morphometry

During recordings, PVN neurones were intracellularly filled with biocytin (0.2%), and then stained with the avidin–biotin complex (ABC)–diaminobenzidine tetrahydrochloride (DAB) as previously described (Stern, 2001; Sonner & Stern, 2007). Slices were fixed overnight in a 4% paraformaldehyde–0.2% picric acid solution,

© 2008 The Authors. Journal compilation © 2008 The Physiological Society

dissolved in 0.3 M phosphate buffered saline (PBS; pH ~7.3) and thoroughly rinsed with 0.01 M PBS. Slices were incubated in 10% normal horse serum, thoroughly rinsed with 0.01 M PBS and overnight in ABC (Vector Laboratories) diluted 1 : 100, and reacted with DAB (60 mg (100 ml)$^{-1}$). Sections were rinsed in 0.01 M PBS, mounted, and dried (Stern, 2001). For morphometric analysis, the entire somatic and dendritic compartments were reconstructed three-dimensionally using a tracing system (Neurolucida, Microbrightfield). Reconstructions were performed using a ×60 oil objective, and the course of each dendrite was traced by digitizing the $X$, $Y$ and $Z$ coordinates as well as its width. Several parameters, including dendritic length, surface area and volume were calculated by algorithms provided by Neurolucida. Axons were identified by their thinner diameter and beaded appearance, and were artificially cut at the slice surface (Stern, 2001). Damaged (e.g. somatic swelling, missing or cut dendritic trees) or weakly labelled neurones were not included in the analysis (Stern, 2001). Data were not corrected for tissue shrinkage, and thus this may underestimate true values affected by shrinkage.

### Chemicals

All chemicals were obtained from Sigma-Aldrich (St Louis, MO, USA), with the exceptions of pyruvic acid (MP Biomedicals, Aurora, OH, USA) and TTX (Alomone Laboratories, Jerusalem, Israel).

### Statistical analysis

All values are expressed as means ± S.E.M. In most cases, Student's $t$ test for unpaired or paired data was used, as indicated. When needed, a two-way ANOVA with a Bonferroni *post hoc* test was used, as indicated. Differences were considered statistically significant at a $P < 0.05$. All statistical analyses were conducted using the same statistical software, GraphPad Prism (GraphPad Software, San Diego, CA, USA).

## Results

Whole-cell patch clamp recordings were obtained from retrogradely labelled PVN-RVLM neurones in sham ($n = 43$) and hypertensive ($n = 43$) rats. Mean values of systolic blood pressure at the sixth–seventh week post-surgery were 120.7 ± 4.1 mmHg and 196.7 ± 9.2 mmHg, respectively ($P < 0.0001$).

The mean neuronal input resistance was 1226.0 ± 170.8 MΩ and 1178.0 ± 109.4 MΩ for sham and hypertensive PVN-RVLM neurones, respectively ($P > 0.8$). Neuronal cell capacitance was significantly reduced in PVN-RVLM neurons from hypertensive rats (sham: 27.92 ± 1.37 pF; hypertensive: 23.05 ± 1.31 pF, $P = 0.01$).

### Changes in PVN-RVLM neuronal morphometry in 2K1C hypertensive rats

Cell capacitance is a general indicator of neuronal surface membrane (Hamill *et al.* 1981; Lindau & Neher, 1988). Thus, changes in cell capacitance in hypertensive rats may be indicative of somatodendritic structural changes during this condition. To determine if this was the case, a subset of recorded neurones that were properly filled with biocytin ($n = 24$ and 27 in sham and hypertensive rats) were reconstructed in three dimensions to compare for differences and/or changes in somatic/dendritic surface area among groups (Methods). Results are summarized in Fig. 1. Overall neuronal surface area was significantly reduced in PVN-RVLM neurons in hypertensive rats ($P < 0.05$). While a tendency for reduced somatic area was observed ($P = 0.07$), our results suggest that the reduced neuronal size was mostly due to a significant reduction in dendritic surface area ($P = 0.02$). A similar degree of reduction in total and dendritic surface area was observed in neurones located in the ventromedial (VM) ($n = 10$ in each sham and hypertensive group) and posterior (PaPo) ($n = 9$ in each sham and hypertensive group) subnuclei (results not shown).

### $I_A$ voltage-dependent activation properties

We first compared the $I_A$ activation curves ($n = 27$ and 20 in sham and hypertensive rats). As shown in Fig. 2*B*, $I_A$ activation was significantly reduced in PVN-RVLM neurons from hypertensive rats ($F = 37.2$, $P < 0.0001$, 2-way ANOVA). Distribution histograms of the maximal evoked $I_A$ in sham and hypertensive rats were built and best fitted by a single Gaussian function ($R^2$: 0.81 and 0.97 in sham and hypertensive rats, respectively) (Fig. 2*B*, inset). A significant shift towards lower current amplitude values was observed in neurones from hypertensive rats ($P < 0.02$, Kolmogorov-Smirnov test). Furthermore, a similar degree of reduction in the maximal evoked $I_A$ in hypertensive rats was observed in neurones located in the VM and PaPo subnuclei (not shown).

Based on the differences found in cell size/morphometry between groups (see above), we addressed whether changes in current amplitude in hypertensive rats persisted after being normalized by cell size (i.e. current density, Fig. 2*C*). Our results indicate no differences in PVN-RVLM $I_A$ current density between sham and hypertensive rats ($F = 1.4$, $P > 0.2$, 2 way ANOVA). No differences in $I_A$ activation threshold nor in the half-activation potential were observed between sham and hypertensive rats ($P > 0.5$ in both cases) (Fig. 2*D*). Similarly, no differences

© 2008 The Authors. Journal compilation © 2008 The Physiological Society

in the slope factor ($k$) of the voltage-dependent activation curve, which describes the steepness of the activation curve (voltage sensitivity), were observed between groups ($P > 0.5$). Finally, no differences in the rate of activation of $I_A$, calculated as the 10–90% rise time following a command potential to −10 mV, were observed between the two groups ($P = 0.9$).

To determine whether changes in $I_A$ properties of hypertensive rats were specific to PVN-RVLM neurones, or alternatively, whether they affected other preautonomic cell populations, we obtained recordings from identified PVN neurones that innervate the dorsal vagal complex (DVC), as a control group. PVN-DVC neurones comprise a heterogeneous population that innervates both the nucleus of the solitary tract (NTS) and the dorsal motor nucleus of the vagus (Kannan & Yamashita, 1983; Gardiner & Bennett, 1986; Smith & Ferguson, 1996; Duan *et al.* 1999). Results are summarized in Fig. 3. Differently from PVN-RVLM neurons, no structural morphometric changes were observed in PVN-DVC neurones obtained from hypertensive rats (Fig. 3*B*). Nonetheless, and similar to PVN-RVLM neurones, $I_A$ activation was significantly reduced in PVN-DVC neurones from hypertensive rats ($F = 87.6$, $P < 0.0001$, 2-way ANOVA). Since no differences in cell size were observed between sham and hypertensive rats, $I_A$ current density was also diminished in PVN-DVC neurones from hypertensive rats ($F = 61.0$, $P < 0.0001$, 2-way ANOVA).

### $I_A$ voltage-dependent inactivation properties

The voltage-dependent and kinetic properties of inactivation of $I_A$ were studied in 25 sham and 18 hypertensive PVN-RVLM neurones. Results are summarized in Fig. 4. Overall, $I_A$ steady state inactivation was found to be significantly increased in PVN-RVLM neurones from hypertensive rats ($F = 37.8$, $P < 0.0001$, 2 way ANOVA). Moreover, the mean half-inactivation potential ($V_{1/2\text{inact}}$, i.e. the $V_m$ at which 50% of the maximum current is inactivated) was significantly shifted to a more hyperpolarized membrane potential (~6 mV) in PVN-RVLM neurones from hypertensive rats ($P < 0.05$). The slope factor ($k$) of the inactivation curve was slightly though significantly increased in PVN-RVLM neurones from hypertensive rats (sham: $12.1 \pm 0.4$ mV; hypertensive: $14.5 \pm 0.6$ mV ($P < 0.01$). Finally, no differences in $I_A$ rate of inactivation ($\tau$) were observed between groups ($P > 0.5$).

### Recovery of $I_A$ from Inactivation

The rate of $I_A$ recovery from inactivation was determined in 20 sham and 12 hypertensive PVN-RVLM neurones. A progressively larger amount of $I_A$ activation was achieved following hyperpolarizing pulses of increasing durations (−100 mV, 10–250 ms, in 10 ms increments), followed by a command potential to −10 mV (Fig. 5*A*), supporting

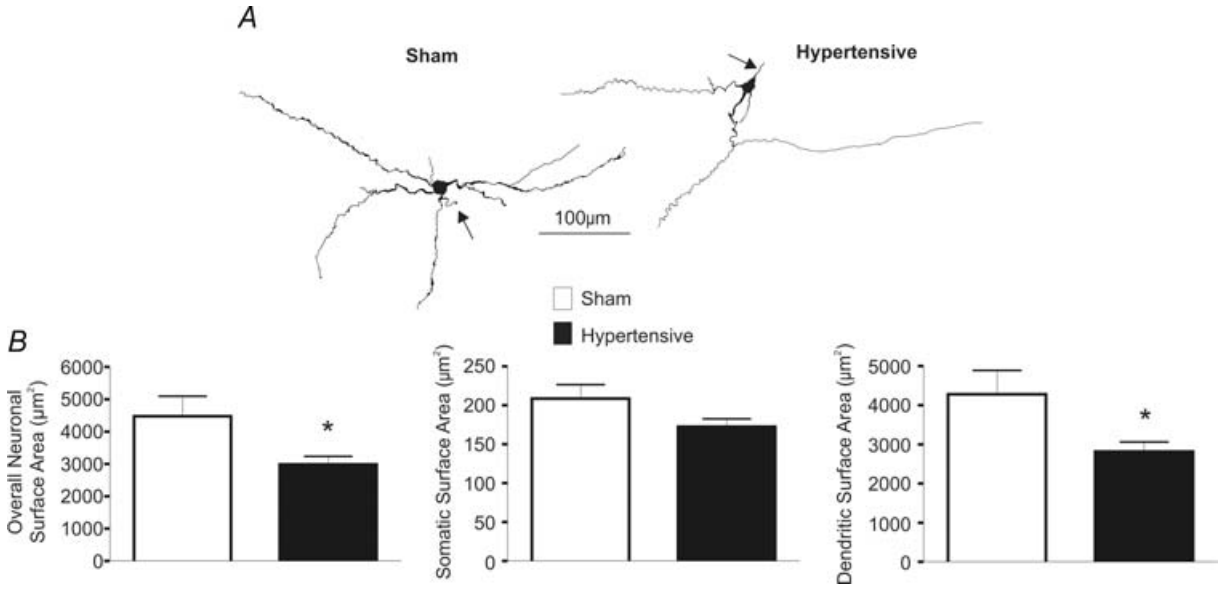


**Figure 1. Changes in PVN-RVLM neuronal morphometry in 2K1C hypertensive rats**
*A*, representative examples of reconstructed PVN-RVLM neurones in sham and hypertensive rats. Axons are identified with arrows. *B*, summary data of overall neuronal, somatic and dendritic surface areas ($n = 24$ sham and 27 hypertensive neurones). Note the reduction in the overall neuronal and dendritic surface area in PVN-RVLM neurones in hypertensive rats. *$P < 0.05$.

© 2008 The Authors. Journal compilation © 2008 The Physiological Society

hyperpolarization-dependent removal of $I_A$ inactivation. Plots of the normalized $I_A$ peak amplitude as a function of the duration of the hyperpolarizing conditioning steps were built, and fitted with a monoexponential function (Fig. 5*B*), to determine the $\tau$ of recovery from inactivation. No significant differences in the mean $\tau$ of recovery from inactivation were observed between PVN-RVLM neurones in sham and hypertensive rats ($P > 0.5$).

### Non-stationary fluctuation analysis of $I_A$ in PVN-RVLM neurones: changes in 2K1C hypertensive rats

To determine whether changes in single channel properties contributed to the diminished $I_A$ current observed in hypertensive rats (see above), we used non-stationary fluctuation analysis, a method originally described by Sigworth (1980, 1981). This approach enables the extraction of single-channel information

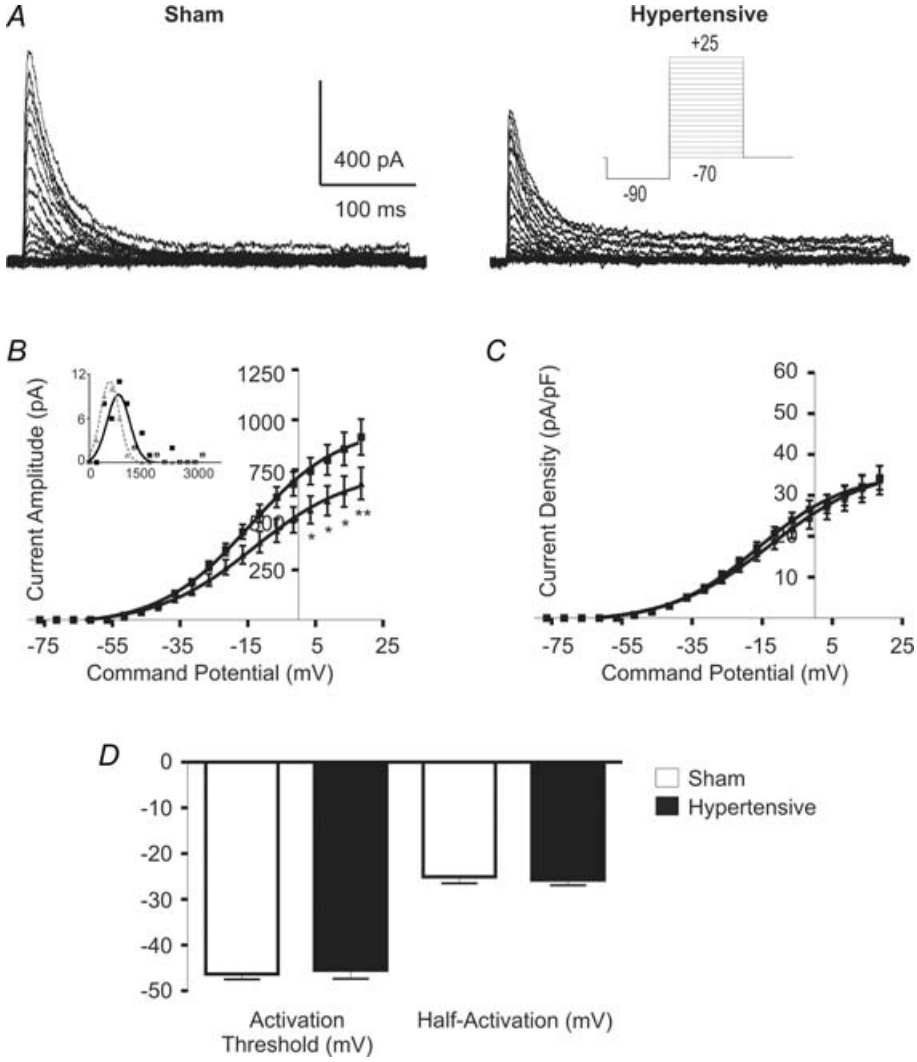


**Figure 2. Changes in $I_A$ voltage-dependent activation properties in 2K1C hypertensive rats**
*A*, representative example of $I_A$ voltage-dependent activation in PVN-RVLM neurones obtained from a sham and a hypertensive rat. Note the smaller maximum current amplitude in the latter. *B*, mean plots of current amplitude *versus* the command potential fitted with Boltzmann functions. Squares and triangles represent sham and hypertensive rats, respectively ($n = 27$ and 20, respectively). Note the significant reduction of $I_A$ magnitude in neurones from hypertensive rats. Inset, distribution histogram of maximal evoked $I_A$ in neurones from sham (squares) and hypertensive (triangles) rats. *Y* and *X* axes: number of neurons and current (pA), respectively. *C*, mean plots of $I_A$ current density *versus* the command potential fitted with Boltzmann functions. Note the lack in reduction of $I_A$ current density in PVN-RVLM neurones from hypertensive rats. *D*, summary data of $I_A$ activation threshold and half-activation potential. No significant differences were observed among the experimental groups. $^*P < 0.05$, $^{**}P < 0.01$.

© 2008 The Authors. Journal compilation © 2008 The Physiological Society

from macroscopic currents, including unitary current, open probability and number of channels. Traces of $I_A$ ($n = 100$–130 traces) evoked with a command pulse to +40 mV were obtained and variance–amplitude relationships were plotted and fitted with a parabolic function (Methods). A representative example is shown in Fig. 6. In most cases, experimental points over the right side of the parabola were missing, indicating that channel open probability never reached a value of 1.0, which is likely to be due to channel inactivation (Sigworth, 1980, 1981; Alvarez *et al.* 2002). Under this condition, we were limited to estimate the unitary current ($i$), determined by the slope of the parabola, shown to be highly accurate even at limited levels of open probability. On the other hand, the number of channels can only be accurately estimated at an open channel probability near 1 (Sigworth, 1980, 1981; Alvarez *et al.* 2002). As shown in Fig. 6*C*, our results indicate a significantly diminished $I_A$ single channel conductance in PVN-RVLM neurones from hypertensive rats ($P < 0.05$).

To support the validity of the non-stationary analysis, we took two complementary approaches. Firstly, we assessed the effects of low-pass filtering the whole-cell currents at different frequencies (100 HZ and 50 Hz). As expected, and recently shown by Villarroel (1997), low-pass filtering reduced the amplitude of the current fluctuations, decreasing the estimated single channel conductance as

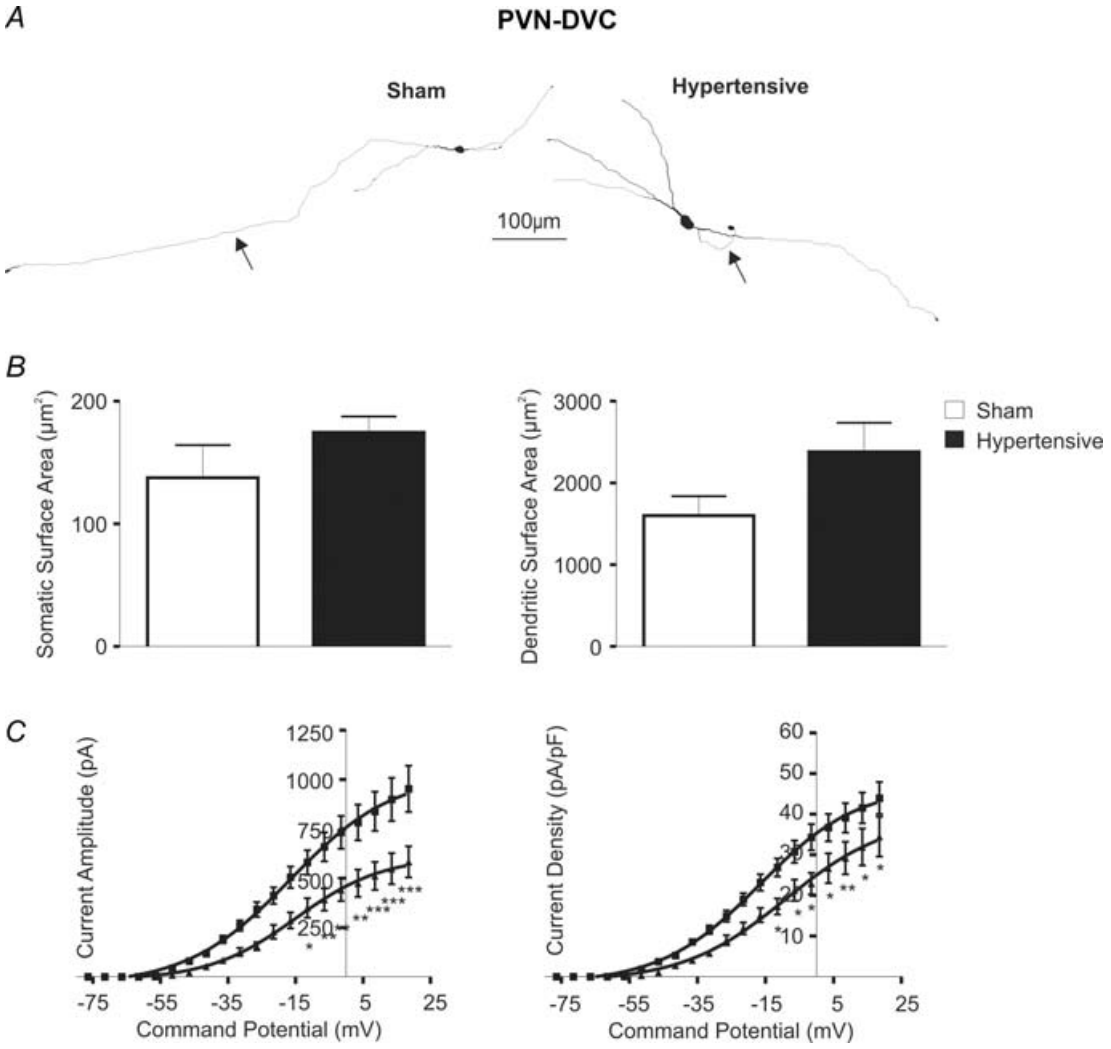


**Figure 3. Morphometric and state-dependent differences in $I_A$ voltage-dependent activation properties of PVN-DVC neurones**

*A*, representative examples of reconstructed PVN-DVC neurones in sham and hypertensive rats. Axons are identified with arrows. *B*, summary data of somatic and dendritic surface area. Note the lack of changes in hypertensive rats. *C*, mean plots of the current amplitude and current density *versus* the command potential fitted with Boltzmann functions. Squares and triangles represent sham and hypertensive rats, respectively ($n = 18$ and 14, respectively). Note the significant reduction of $I_A$ amplitude and current density in hypertensive rats. $^*P < 0.05$, $^{**}P < 0.01$, $^{***}P < 0.0001$.

© 2008 The Authors. Journal compilation © 2008 The Physiological Society

the filter frequency was reduced (100 Hz: 84.1 ± 4.1% of theoretical; 50 Hz: 79.8 ± 4.8% of theoretical; $n = 6$, $P < 0.001$ repeated measures ANOVA). Secondly, we found that low concentrations of 4-AP (1–2 mM), known to diminish open channel probability without affecting channel conductance (Yao & Tseng, 1994), diminished whole $I_A$ current without affecting estimated single channel conductance (control: 21.3 ± 5.9 pS; 4-AP: 21.4 ± 6.0 pS; $n = 3$, $P > 0.7$).

### The $Na^+$ action potential waveform is affected in PVN-RVLM neurones in 2K1C hypertensive rats

Abundant evidence supports a major role for $I_A$ in the regulation of single and repetitive neuronal firing behaviour (Connor & Stevens, 1971; Rudy, 1988; Serodio & Rudy, 1998; Kim *et al.* 2005). Thus, we evaluated whether action potential properties known to be affected by $I_A$ are altered in PVN-RVLM neurones from hypertensive rats. In a first series of studies, we evaluated differences in the single action potential waveform. Individual action potentials were evoked using short (5 ms) depolarizing pulses, while injecting current to maintain $V_m$ at approximately two different membrane potentials (∼ −80 mV and ∼ −50 mV, see Methods), in order to obtain different degrees of $I_A$ inactivation. In PVN-RVLM neurones from sham rats, action potentials evoked from a more depolarized $V_m$ (∼ −50 mV) were wider (by ∼177.5 ± 16.3%, $P < 0.001$) and displayed a slower decay time course when compared to spikes evoked at a $V_m$ of ∼ −80 mV (by 160.0 ± 23.3%, $P < 0.05$). These differences were likely to be due to a higher degree of $I_A$ inactivation at the more depolarized $V_m$, as we recently reported (Sonner & Stern, 2007). At a membrane potential of ∼ −80 mV, action potentials in PVN-RVLM neurons from hypertensive rats were wider and decayed slower than those evoked in sham rats at a similar $V_m$ ($P < 0.05$ in both cases). Spike width in hypertensive rats was further increased at a $V_m$ of ∼ −50 mV (151.3 ± 11.0%, $P < 0.05$), though to a lesser extent than that observed in sham rats (see above). Moreover, the decay time course at ∼ −50 mV was not significantly different from that observed at ∼ −80 mV ($P > 0.5$). Results are summarized in Fig. 7*A*.

As we previously reported (Sonner & Stern, 2007), 4-AP, a $K^+$ channel blocker that more selectively blocks $I_A$ over other voltage-dependent $K^+$ channels (e.g. $IK_{DR}$), prolonged the action potential width and slowed down the decay time course in PVN-RVLM neurones, effects that were significantly diminished in hypertensive rats (spike width – sham: 243.4 ± 17.2%; hypertensive: 176.4 ± 16.9%; decay time – sham: 285.0 ± 27.4%; hypertensive: 190.9 ± 24.7%; $P < 0.05$ in both cases, paired *t* test). Moreover, in the presence of 4-AP, differences in spike width or decay time were no longer observed between sham and hypertensive rats ($P > 0.5$, not shown).

To determine whether the action potential waveform during repetitive firing activity in PVN-RVLM

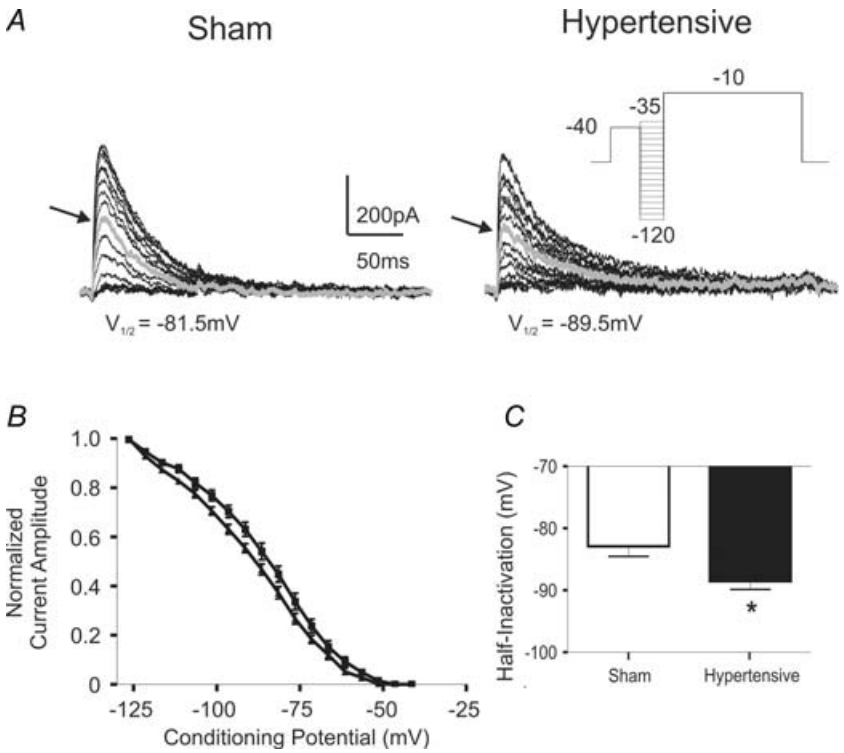


**Figure 4. Changes in $I_A$ voltage-dependent inactivation properties in PVN-RVLM neurones in 2K1C hypertensive rats**
*A*, representative traces of the voltage dependence of inactivation of $I_A$ in sham and hypertensive rats. The grey traces (arrow) represent the current evoked at the half-inactivation potential (values listed under the traces). *B*, plots of mean normalized current amplitude *versus* the conditioning potential fitted by Boltzmann functions. Note the hyperpolarizing shift in PVN-RVLM neurones from hypertensive rats. Squares and triangles represent sham and hypertensive rats, respectively ($n = 25$ and 18, respectively). *C*, summary data of $I_A$ half-inactivation potential. *$P < 0.05$.

© 2008 The Authors. Journal compilation © 2008 The Physiological Society

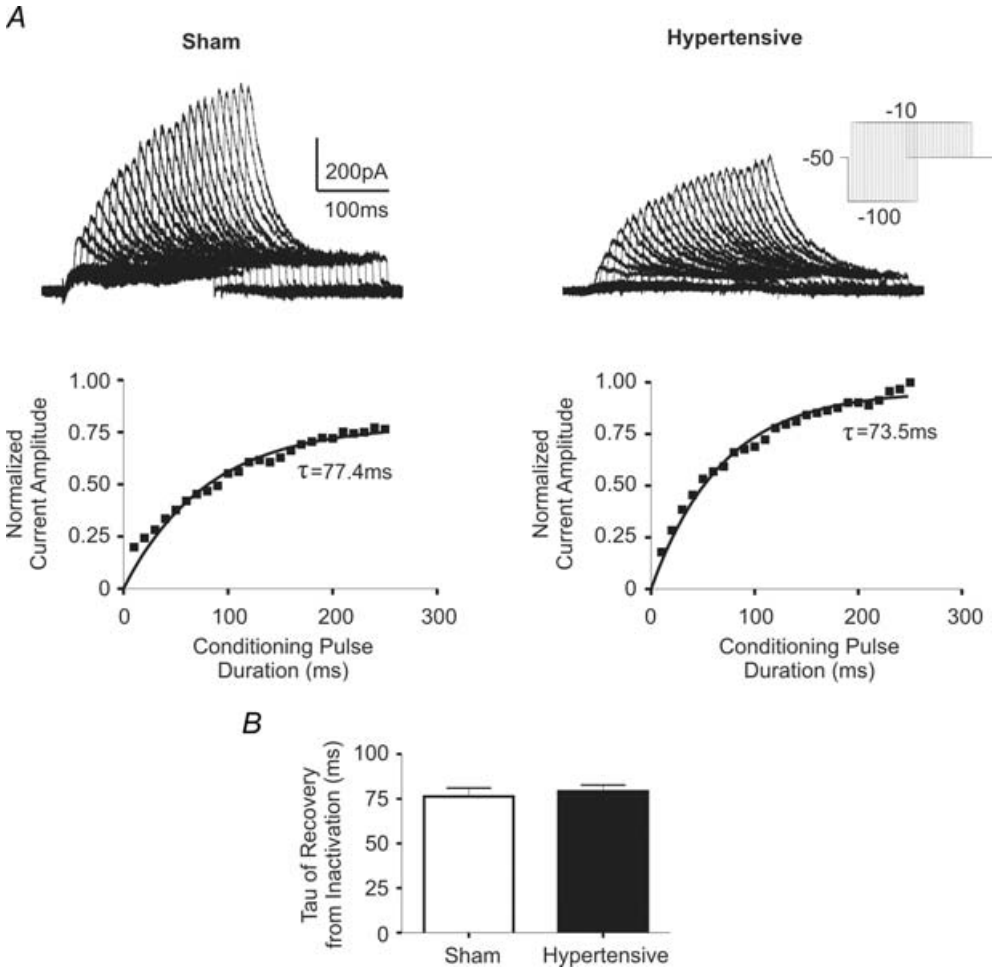


**Figure 5. Time course of recovery from inactivation of $I_A$ in PVN-RVLM neurones in sham and hypertensive rats**
*A*, representative traces of $I_A$ currents evoked from a command pulse of −10 mV with a conditioning pulse (−100 mV) of increasing duration (10–250 ms, Δ10 ms increments). Lower panels depict the normalized current amplitude evoked at the command test, plotted against the conditioning step duration. A single exponential function was fitted to the plot, and the time course of recovery from inactivation ($\tau$) of $I_A$ was calculated. The time constant ($\tau$) of recovery from inactivation is listed below each trace. *C*, summary data of mean $\tau$ of recovery from inactivation ($n = 20$ sham and 12 hypertensive neurones). No significant differences were observed between groups.

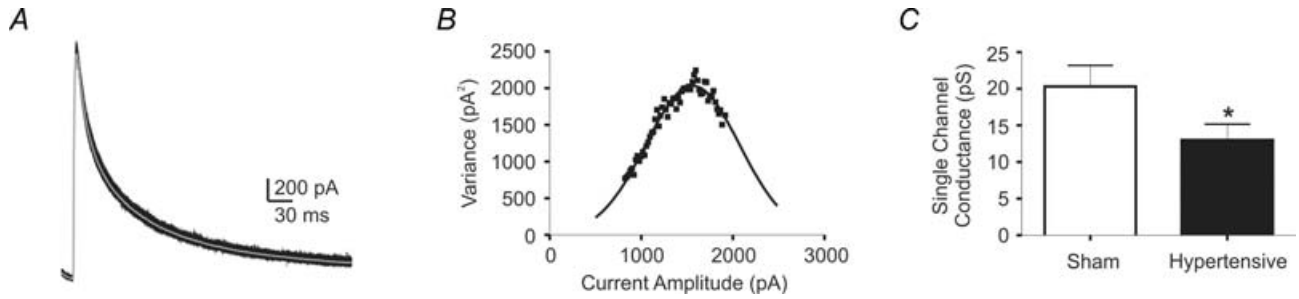


**Figure 6. Non-stationary noise analysis of $I_A$ in PVN-RVLM neurones of sham and hypertensive rats**
*A*, representative traces of $I_A$ evoked with a command potential to +40 mV. The grey trace is the mean evoked current. *B*, plot of the variance as a function of the current amplitude obtained from the same representative traces in *A*. The plot was fitted with a parabolic function. *C*, summary data of mean single channel conductance in sham and hypertensive rats ($n = 12$ and 9, respectively). Note the significantly reduced single channel conductance in the hypertensive neurones. $^*P < 0.05$.

© 2008 The Authors. Journal compilation © 2008 The Physiological Society

neurones was also altered in hypertensive rats, action potentials from spontaneously active neurones ($n = 9$ and 12 in sham and hypertensive rats, respectively) were grouped and compared between experimental groups (Methods). Representative examples are shown in Fig. 7*B*. Spontaneous firing activity was significantly higher in PVN-RVLM neurones from hypertensive rats ($P < 0.01$). Similarly to the differences observed on single evoked spikes, spontaneous action potentials in hypertensive rats were wider ($P < 0.05$) and displayed a slower decay time course ($P < 0.005$) than those recorded from sham rats. Moreover, the slope of the hyperpolarizing after-potential (HAP) following each spike was significantly steeper in PVN-RVLM neurones from hypertensive rats ($P < 0.01$). Altogether, these data support a diminished $I_A$ influence in the regulation of the action potential

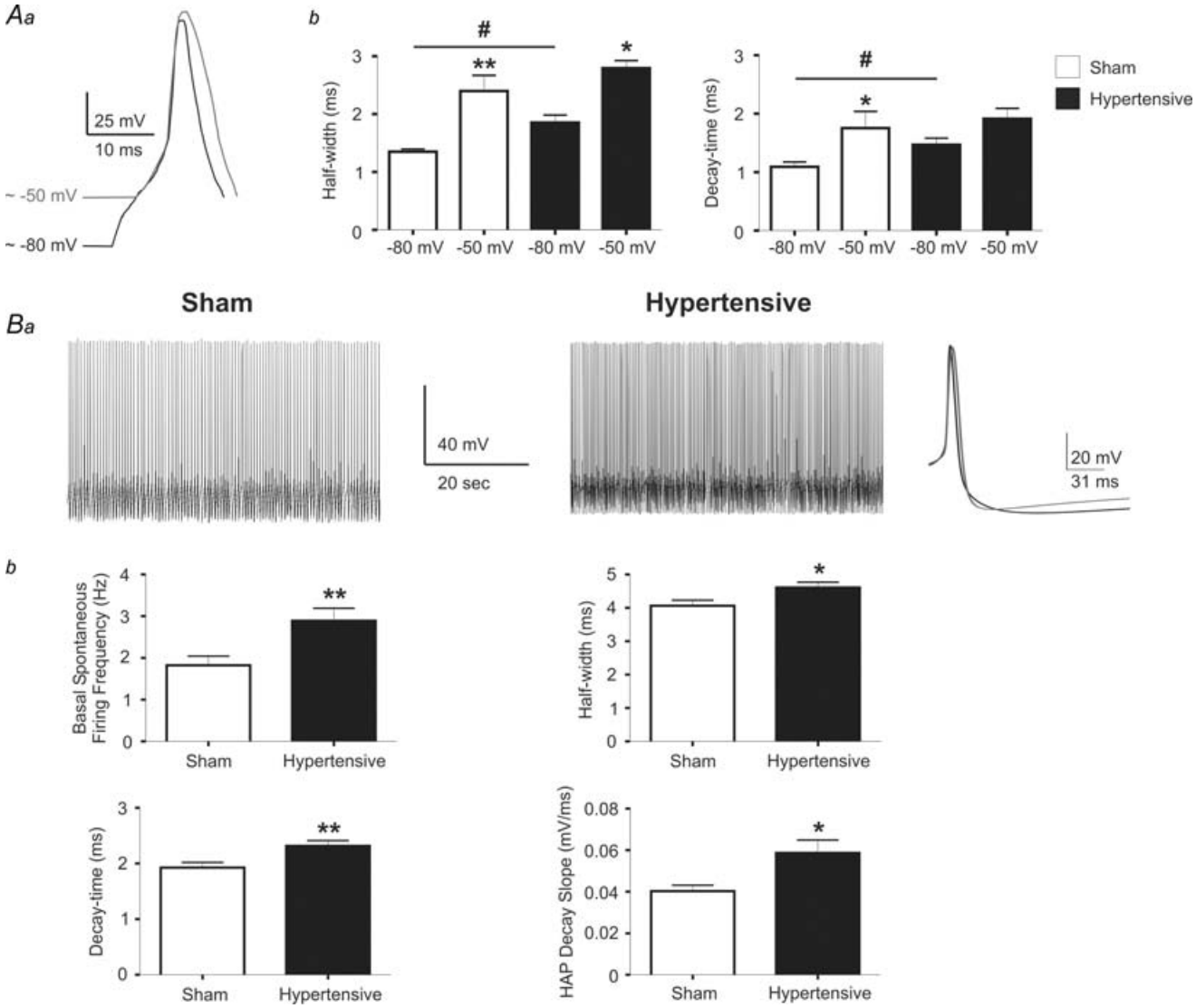


**Figure 7. Changes in $Na^+$ action potential waveform of PVN-RVLM neurones in 2K1C hypertensive rats**
*Aa*, representative traces of evoked action potentials at a membrane potential $\sim -80$ mV (black trace) and $\sim -50$ mV (grey trace) in a PVN-RVLM neurone from a sham rat. Action potentials were aligned to better depict differences in their waveforms. *b*, summary data of evoked action potential half-widths and decay times at membrane potentials of $\sim -80$ mV and $\sim -50$ mV ($n = 9$ sham and 12 hypertensive neurones). $^*P < 0.05$ and $^{**}P < 0.01$ (sham $-50$ mV *versus* sham $-80$ mV); $\#P < 0.05$ (sham $-80$ mV *vs*. hypertensive $-80$ mV). *Ba*, representative traces of spontaneous firing activity in PVN-RVLM neurones from a sham and a hypertensive rat. The averaged spontaneous action potential from the sham (black trace) and the hypertensive (grey) rat were superimposed and shown in the right panel. *b*, summary data of basal spontaneous firing activity, half-width, decay-time, and HAP decay slope from the averaged spontaneous single spikes ($n = 9$ sham and 12 hypertensive neurones). $^*P < 0.05$, $^{**}P < 0.01$.

© 2008 The Authors. Journal compilation © 2008 The Physiological Society

waveform in PVN-RVLM neurones from hypertensive rats.

### Action potential-dependent increase in intracellular $Ca^{2+}$ is enhanced in PVN-RVLM neurons from 2K1C hypertensive rats

Since an increase in spike duration is known to be associated with an increase in intracellular calcium levels (Kirkpatrick & Bourque, 1991), we combined simultaneous patch clamp recordings and confocal $Ca^{2+}$ imaging in order to determine if action potential-evoked changes in intracellular calcium levels ($[Ca^{2+}]_{ic}$) were altered in hypertensive rats. Retrogradely labelled PVN-RVLM neurones were intracellularly filled with Fluo-5F (100 $\mu$M), and relative changes in $[Ca^{2+}]_{ic}$ in response to single evoked action potentials were measured (Methods, Fig. 8*A* and *B*), and between 8 and 10 traces of calcium transients were averaged in order to increase the signal to noise ratio. The peak of the $[Ca^{2+}]_{ic}$ transient evoked from a single spike was measured before and after 5 mM 4-AP application in PVN-RVLM neurones from sham ($n = 9$) and hypertensive ($n = 11$) rats. Results are summarized in Fig. 8*C*. Action potential-evoked $[Ca^{2+}]_{ic}$ transients in PVN-RVLM neurons from hypertensive rats were significantly larger than those evoked in sham rats ($P < 0.05$). Moreover, while 4-AP significantly enhanced the $Ca^{2+}$ transient in the sham group (78.1 ± 19.3%, $P < 0.05$), it failed to do so in the hypertensive group ($P > 0.05$) (Fig. 8*C*).

### Spike broadening during repetitive firing is enhanced in PVN-RVLM neurones in 2K1C hypertensive rats

Repetitive firing activity of PVN neurones, including identified preautonomic neurones, is characterized by a progressive increment in action potential duration (spike broadening) (Bains & Ferguson, 1999; Stern, 2001), a phenomenon shown to be dependent on progressive increment in $[Ca^{2+}]_{ic}$ and steady-state inactivation of $I_A$ (Hlubek & Cobbett, 2000). Thus, we explored whether spike broadening in PVN-RVLM neurones was also

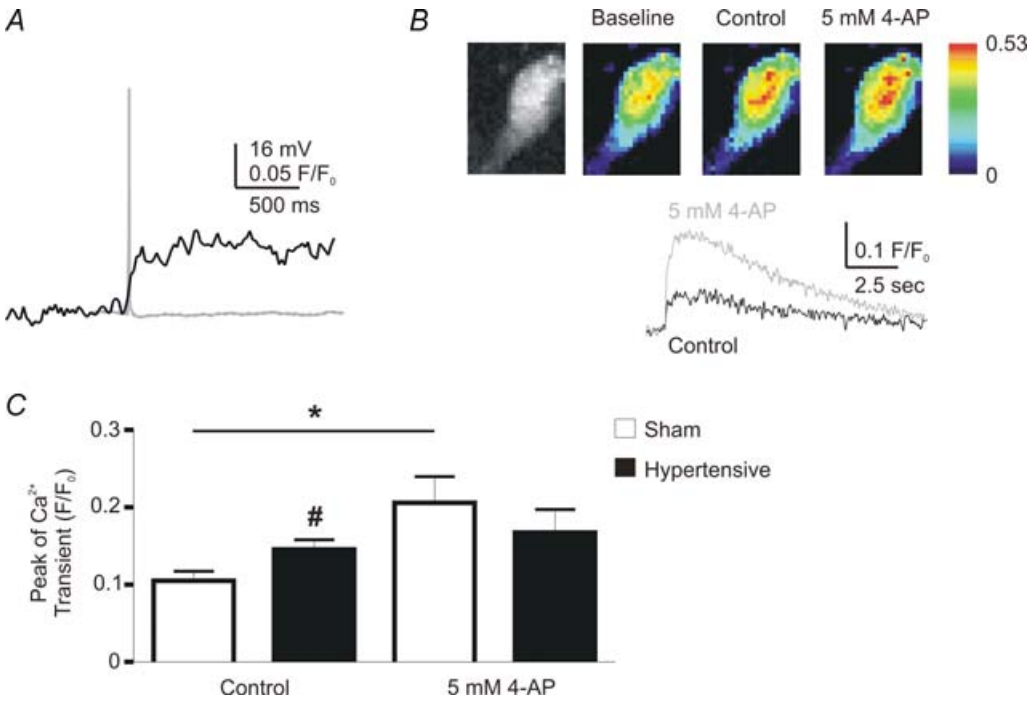


**Figure 8. Changes in action potential-evoked $[Ca^{2+}]_{ic}$ levels in PVN-RVLM neurones in 2K1C hypertensive rats**

*A*, representative traces of an evoked action potential (grey) and the resultant change in $[Ca^{2+}]_{ic}$ levels (black) in a sham rat. *B*, representative confocal images showing a Fluo-5 loaded PVN-RVLM neurone (left panel), as well as basal and peak action potential-evoked $[Ca^{2+}]_{ic}$ levels (pseudocolor images) in the absence and presence of 5 mM 4-AP (scale units are $F/F_0$). The lower traces show the time course of changes in the action potential-evoked $[Ca^{2+}]_{ic}$ in control (black trace) and in the presence of 4-AP (grey trace). Note the increase in the magnitude of the $[Ca^{2+}]_{ic}$ transient in the presence of 4-AP. *C*, summary data of the peak of the $[Ca^{2+}]_{ic}$ transient, before and after 4-AP, in sham and hypertensive neurones ($n = 9$ and 11, respectively). *$P < 0.05$ (sham control *versus* sham 4-AP); #$P < 0.05$ (sham control *versus* hypertensive control).

© 2008 The Authors. Journal compilation © 2008 The Physiological Society

affected in hypertensive rats. Repetitive firing was evoked with depolarizing pulses (110–130 pA, 180 ms), and the spike width of the evoked action potentials was measured and compared between groups. The degree of spike broadening was quantified as the ratio of the duration of the third spike to that of the first spike during the train (Shao *et al.* 1999; Stern, 2001). Representative examples and summary data are shown in Fig. 9. While spike broadening was observed in both groups, the degree of broadening was significantly larger in PVN-RVLM neurones from hypertensive rats ($P < 0.05$).

## Discussion

### Changes in $I_A$ properties and structural plasticity in PVN-RVLM neurones in 2K1C hypertensive rats

Our results indicate an overall reduction in the magnitude of the evoked $I_A$ in PVN-RVLM neurones from hypertensive rats. While differences were observed at relatively depolarized membrane potentials (see Fig. 2*B*), these were within the range of membrane potentials reached during action potential firing. Thus, changes in $I_A$ magnitude in hypertensive rats observed under our voltage-clamp experimental conditions would be expected to have a functional impact under more physiological conditions. This is in fact supported by our studies on single and repetitive action potential firing properties, as discussed below.

A similar degree of diminished $I_A$ was observed among PVN-RVLM neurones located in different subnuclei (i.e. VM and PaPo), as well as in PVN-DVC neurons, suggesting that changes in $I_A$ in renovascular hypertensive rats may occur in a relatively homogeneous manner within preautonomic PVN neurones. Additional studies including further identified PVN neuronal populations (e.g. spinally projecting, neurosecretory) will be needed to more conclusively assess the extent of changes in $I_A$ within discrete PVN neuronal populations in renovascular hypertension.

In addition to changes in current amplitude, some critical voltage-dependent properties of $I_A$ were also altered in hypertensive rats, which could in turn contribute to changes in the magnitude/availability of $I_A$. For example, the degree of $I_A$ steady-state inactivation was enhanced in PVN-RVLM neurones from hypertensive rats, and a hyperpolarizing shift in the $V_{1/2}$ inactivation was also observed in this condition. Similar changes in $I_A$ inactivation properties were previously reported in peripheral sympathetic neurons in the spontaneously hypertensive rat (Robertson & Schofield, 1999). An increased degree of steady-state inactivation in hypertensive rats indicates that at a particular membrane potential, fewer channels will be available for activation. Thus, the larger degree of voltage-dependent inactivation of $I_A$ may be a contributing factor to the reduced magnitude of the evoked $I_A$ in hypertensive rats.

Another potential mechanism contributing to diminished $I_A$ availability in hypertensive rats is a reduction in single channel conductance. Our results using non-stationary noise analysis support a diminished single channel conductance of A-type $K^+$ channels in hypertensive rats. These results, however, need to be interpreted cautiously, since they constitute an indirect estimation of single channel properties based on fluctuations obtained from whole cell currents. Nonetheless, this analysis has been extensively used to estimate single channel properties in various cell types (Moran & Conti, 1990; Yoshimura *et al.* 1999; Li & Correa, 2002; Hartveit & Veruki, 2006). Further supporting the validity of this approach in our experimental conditions, we found the values for A-type $K^+$ single channel conductance to be in general agreement with previous reports based on single-channel recordings (Cooper & Shrier, 1985; Kasai *et al.* 1986; Wang *et al.* 1997; Kang *et al.* 2000).

Concomitant with a decreased $I_A$ magnitude in hypertensive rats, we found PVN-RVLM neurones to display a

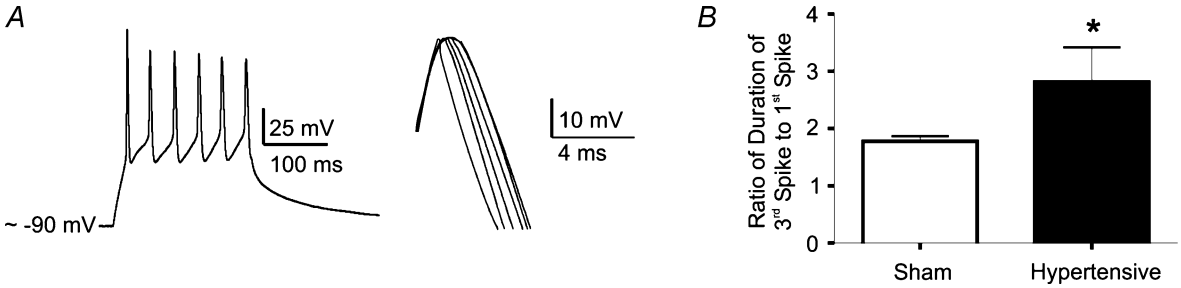


**Figure 9. Changes in spike broadening in PVN-RVLM neurones in 2K1C hypertensive rats**
*A*, representative trace of an evoked burst of spikes (110 pA, 180 ms) in a PVN-RVLM neurone from a sham rat (left panel). In the right panel, the evoked spikes were scaled and superimposed to better depict the progressive increase in width. *B*, mean ratio of the half-width of the third spike to that of the first spike. Note the significantly increased ratio in the hypertensive group ($n = 22$ and 15 in sham and hypertensive rats, respectively). $^*P < 0.05$.

© 2008 The Authors. Journal compilation © 2008 The Physiological Society

significantly reduced dendritic surface area in hypertensive rats. As a consequence, $I_A$ current density (i.e. the current normalized by cell size) was not changed in hypertensive rats. At present, however, it cannot be determined whether changes in $I_A$ magnitude are independent or compensatory to changes in neuronal size. The fact that a similar decrease in $I_A$ amplitude was observed in PVN-DVC neurones in the absence of changes in cell size, would suggest that changes in $I_A$ and neuronal morphometry in hypertensive rats are independent events. It is worth mentioning that the diminished single channel conductance, along with an enhanced voltage-dependent channel inactivation, would be expected to result in a diminished current density. While we currently lack an explanation for this apparent discrepancy, it cannot be ruled out that multiple opposing and/or compensating changes in $I_A$ occur in hypertensive rats (e.g. diminished single channel conductance along with increased open channel probability or increased total number of channels) (Robertson & Schofield, 1999), such that current density remains unchanged.

### Changes in action potential waveform, action-potential-dependent $Ca^{2+}$ transients and repetitive firing properties in PVN-RVLM neurones in 2K1C hypertensive rats

Based on its subthreshold availability and rapid kinetics of activation, $I_A$ is well positioned to influence $Na^+$ action potential properties (in particular action potential width and decay time course) in numerous cell types (Rogawski, 1985; Rudy, 1988; Li & Ferguson, 1996; Magee *et al.* 1998; Luther & Tasker, 2000; Sonner & Stern, 2007), including PVN-RVLM neurons, as we recently showed (Sonner & Stern, 2007). The wider and more slowly decaying action potentials observed in PVN-RVLM neurones from hypertensive rats are consistent with a diminished $I_A$ availability during this condition. This is also supported by the fact that in hypertensive rats, two interventions that diminish $I_A$ availability (i.e. membrane depolarization and the A-type $K^+$ channel blocker 4-AP (Sonner & Stern, 2007) were blunted. Our studies also indicate an increased degree of PVN-RVLM spontaneous firing discharge in renovascular hypertensive rats, as recently shown in spontaneously hypertensive rats (Li & Pan, 2006). While spontaneous firing activity in the slice preparation likely does not reflect the one that may be observed in the whole animal, in which extrinsic inputs are intact, the increased degree of activity reported herein further supports a contribution of intrinsic mechanism to increased excitability in renovascular hypertensive rats.

Voltage-gated $Ca^{2+}$ channels are activated during action potentials, resulting in an influx of $Ca^{2+}$ and subsequent activation of $Ca^{2+}$-dependent signalling mechanisms (Kirkpatrick & Bourque, 1991; Hlubek & Cobbett, 2000). The spike duration is an important parameter regulating the amount of $Ca^{2+}$ entry with each spike (Stewart & Foehring, 2001). Thus, we hypothesized that prolongation of action potential duration due to diminished $I_A$ availability in hypertensive rats would result in an enhanced $Ca^{2+}$ influx per spike. Our results showed that action potential-dependent $Ca^{2+}$ entry was enhanced in PVN-RVLM neurones from hypertensive rats. As previously reported in other neuronal types (Goldberg *et al.* 2003), 4-AP enhanced the action potential-evoked $Ca^{2+}$ transient, an effect that was diminished in hypertensive rats.

Both PVN and SON neurones show a prominent progressive increase in spike duration during repetitive firing (Andrew & Dudek, 1985; Bourque & Renaud, 1985; Bains & Ferguson, 1999; Stern, 2001). Spike broadening is thought to be dependent both on accumulation of intracellular $Ca^{2+}$ and progressive inactivation of $I_A$ (Kirkpatrick & Bourque, 1991; Ma & Koester, 1996; Hlubek & Cobbett, 2000). Consistent with a diminished $I_A$ availability and enhanced action potential-dependent $Ca^{2+}$ transients in hypertensive rats, we found the degree of spike broadening in PVN-RVLM neurones to be enhanced in hypertensive rats.

The precise functional role of spike broadening in PVN-RVLM neurones, as well as the consequence of its potentiation in hypertensive rats is at present uncertain. It is well established that $Ca^{2+}$ influx through voltage-gated $Ca^{2+}$ channels has important implications for many neuronal processes including regulation of $Ca^{2+}$-dependent second messengers and enzymes, gene expression, and neurotransmitter release, among others (Bertolino & Llinas, 1992; Bito *et al.* 1997). For example, at the presynaptic nerve terminal, the width of the action potential determines the amount of transmitter release (Augustine, 1990; Sabatini & Regehr, 1997; Geiger & Jonas, 2000). Because of the very steep $Ca^{2+}$ dependence of neurotransmitter release (Augustine, 1990; Jackson *et al.* 1991), broader spikes in neurones from hypertensive rats would be expected to result in more efficient neurotransmitter release from PVN terminals within the RVLM, as shown in hippocampal neurones (Wheeler *et al.* 1996). This will assume however, that similar channels influencing spike broadening are expressed in somata and terminals in preautonomic PVN neurones. It is worth noting that similar types of $K^+$ channels were shown to regulate spike broadening both at magnocellular neurosecretory somata and pituitary nerve terminals (Jackson *et al.* 1991). Finally, in addition to synaptic facilitation at nerve terminals, broader spikes back-propagating to the dendrites may facilitate the pairing of incoming excitatory postsynaptic potentials and post-synaptic action potentials, a mechanism shown to enhance synaptic efficacy (Magee & Johnston, 1997). Thus, by affecting intrinsic membrane properties and signalling

© 2008 The Authors. Journal compilation © 2008 The Physiological Society

pathways, as well as pre- and postsynaptic efficacy, diminished $I_A$ function and concomitant increases in spike duration and $Ca^{2+}$ influx may constitute important mechanisms underlying enhanced activation and efficacy of the PVN-RVLM pathway in renovascular hypertensive rats. Interestingly, a diminished $I_A$ activity has also been shown to increase excitability in NTS neurones of hypertensive rats (Sundaram *et al.* 1997; Belugin & Mifflin, 2005). Thus, depending on the specific cardiovascular-related neuronal type and/or circuit affected, a diminished $I_A$ activity could either favour (e.g. PVN) or oppose (e.g. NTS) mechanisms contributing to sympathoexcitation and increased blood pressure in hypertensive rats.

### Potential mechanisms leading to altered $I_A$ properties in PVN-RVLM neurons in renovascular hypertension

It is at present unknown what the sources and/or mechanisms leading to diminished $I_A$ activity in PVN-RVLM neurones in renovascular hypertensive rats are. However, due to its importance in renovascular hypertension and sympathoexcitation (Fink, 1997), and the well established inhibitory effect of AngII on $I_A$ within the hypothalamus (Nagatomo *et al.* 1995; Li & Ferguson, 1996; Wang *et al.* 1997), it is reasonable to speculate that AngII-dependent signalling contributes to altered PVN $I_A$ function in renovascular hypertensive rats. Within the PVN, AngII binding to AT1a receptors increase neuronal firing activity (Li & Ferguson, 1993; Cato & Toney, 2005) and sympathetic outflow (Zhu *et al.* 2002; Dampney *et al.* 2005; Li *et al.* 2006). Moreover, abundant evidence supports enhanced PVN AngII activity during hypertension (Gutkind *et al.* 1988; Jung *et al.* 2004; Dampney *et al.* 2005). While activation of AT1a receptors and its downstream neuronal effects are linked to various intracellular signalling pathways (Sumners *et al.* 1996), generation of reactive oxygen species (ROS) is a critical mechanism underlying central sympathoexcitatory and neuronal AngII effects (Zimmerman *et al.* 2002; 2005; Campese *et al.* 2005). In fact, diminished $K^+$ channel activity is commonly observed during enhanced oxidative stress (Liu & Gutterman, 2002; Cogolludo *et al.* 2006), and an AngII-mediated ROS-dependent inhibition of $K^+$ channel activity has been shown in neurones of the hypothalamus and brain stem (Sun *et al.* 2005). In addition, AngII was shown to reduce the expression of Kv4.3 mRNA both in cardiac (Takimoto *et al.* 1997; Zhang *et al.* 2001) and brain (Gao *et al.* 2006) tissues, an effect shown to occur in a ROS-dependent manner (Zhou *et al.* 2006). Thus, future studies are warranted to determine the contribution of the AngII-ROS signalling pathway to diminished $I_A$ function and/or channel expression in PVN neurones in renovascular hypertensive rats.

## References


Allen AM (2002). Inhibition of the hypothalamic paraventricular nucleus in spontaneously hypertensive rats dramatically reduces sympathetic vasomotor tone. *Hypertension* **39**, 275–280.

Alvarez O, Gonzalez C & Latorre R (2002). Counting channels: a tutorial guide on ion channel fluctuation analysis. *Adv Physiol Educ* **26**, 327–341.

Andrew RD & Dudek FE (1985). Spike broadening in magnocellular neuroendocrine cells of rat hypothalamic slices. *Brain Res* **334**, 176–179.

Armstrong WE, Warach S, Hatton GI & McNeill TH (1980). Subnuclei in the rat hypothalamic paraventricular nucleus: a cytoarchitectural, horseradish peroxidase and immunocytochemical analysis. *Neuroscience* **5**, 1931–1958.

Augustine GJ (1990). Regulation of transmitter release at the squid giant synapse by presynaptic delayed rectifier potassium current. *J Physiol* **431**, 343–364.

Bains JS & Ferguson AV (1999). Activation of N-methyl-D-aspartate receptors evokes calcium spikes in the dendrites of rat hypothalamic paraventricular nucleus neurons. *Neuroscience* **90**, 885–891.

Belugin S & Mifflin S (2005). Transient voltage-dependent potassium currents are reduced in NTS neurons isolated from renal wrap hypertensive rats. *J Neurophysiol* **94**, 3849–3859.

Bergamaschi C, Campos RR, Schor N & Lopes OU (1995). Role of the rostral ventrolateral medulla in maintenance of blood pressure in rats with Goldblatt hypertension. *Hypertension* **26**, 1117–1120.

Bertolino M & Llinas RR (1992). The central role of voltage-activated and receptor-operated calcium channels in neuronal cells. *Annu Rev Pharmacol Toxicol* **32**, 399–421.

Bito H, Deisseroth K & Tsien RW (1997). $Ca^{2+}$-dependent regulation in neuronal gene expression. *Curr Opin Neurobiol* **7**, 419–429.

Bourque CW & Renaud LP (1985). Activity dependence of action potential duration in rat supraoptic neurosecretory neurones recorded in vitro. *J Physiol* **363**, 429–439.

Campese VM, Shaohua Y & Huiquin Z (2005). Oxidative stress mediates angiotensin II-dependent stimulation of sympathetic nerve activity. *Hypertension* **46**, 533–539.

Carvalho TH, Bergamaschi CT, Lopes OU & Campos RR (2003). Role of endogenous angiotensin II on glutamatergic actions in the rostral ventrolateral medulla in Goldblatt hypertensive rats. *Hypertension* **42**, 707–712.

Cato MJ & Toney GM (2005). Angiotensin II excites paraventricular nucleus neurons that innervate the rostral ventrolateral medulla: an in vitro patch-clamp study in brain slices. *J Neurophysiol* **93**, 403–413.

Ciriello J, Caverson MM & Calaresu FR (1985). Lateral hypothalamic and peripheral cardiovascular afferent inputs to ventrolateral medullary neurons. *Brain Res* **347**, 173–176.

Cogolludo A, Frazziano G, Cobeno L, Moreno L, Lodi F, Villamor E, Tamargo J & Perez-Vizcaino F (2006). Role of reactive oxygen species in Kv channel inhibition and vasoconstriction induced by TP receptor activation in rat pulmonary arteries. *Ann N Y Acad Sci* **1091**, 41–51.


© 2008 The Authors. Journal compilation © 2008 The Physiological Society

Connor JA & Stevens CF (1971). Prediction of repetitive firing behaviour from voltage clamp data on an isolated neurone soma. *J Physiol* **213**, 31–53.

Cooper E & Shrier A (1985). Single-channel analysis of fast transient potassium currents from rat nodose neurones. *J Physiol* **369**, 199–208.

Coote JH, Yang Z, Pyner S & Deering J (1998). Control of sympathetic outflows by the hypothalamic paraventricular nucleus. *Clin Exp Pharmacol Physiol* **25**, 461–463.

Czyzewska-Szafran H, Wutkiewicz M, Remiszewska M, Jastrzebski Z, Czarnecki A & Danysz A (1989). Down-regulation of the GABA-ergic system in selected brain areas of spontaneously hypertensive rats (SHR). *Pol J Pharmacol Pharm* **41**, 619–627.

Dampney RA, Czachurski J, Dembowsky K, Goodchild AK & Seller H (1987). Afferent connections and spinal projections of the pressor region in the rostral ventrolateral medulla of the cat. *J Auton Nerv Syst* **20**, 73–86.

Dampney RA, Horiuchi J, Killinger S, Sheriff MJ, Tan PS & McDowall LM (2005). Long-term regulation of arterial blood pressure by hypothalamic nuclei: some critical questions. *Clin Exp Pharmacol Physiol* **32**, 419–425.

Davern PJ & Head GA (2007). Fos-related antigen immunoreactivity after acute and chronic angiotensin II-induced hypertension in the rabbit brain. *Hypertension* **49**, 1170–1177.

De Koninck Y & Mody I (1994). Noise analysis of miniature IPSCs in adult rat brain slices: properties and modulation of synaptic $GABA_A$ receptor channels. *J Neurophysiol* **71**, 1318–1335.

DiCarlo SE, Zheng H, Collins HL, Rodenbaugh DW & Patel KP (2002). Daily exercise normalizes the number of diaphorase (NOS) positive neurons in the hypothalamus of hypertensive rats. *Brain Res* **955**, 153–160.

Duan YF, Kopin IJ & Goldstein DS (1999). Stimulation of the paraventricular nucleus modulates firing of neurons in the nucleus of the solitary tract. *Am J Physiol Regul Integr Comp Physiol* **277**, R403–R411.

Earle ML, Boorman R, Takahashi Y & Pittman QJ (1992). Lesions of the paraventricular nucleus alter the development and intensity of chronic renal hypertension. *Can J Physiol Pharmacol* **70**, Avii–Aviii.

Earle ML & Pittman QJ (1995). Involvement of the PVN and BST in 1K1C hypertension in the rat. *Brain Res* **669**, 41–47.

Esler M & Kaye D (1998). Increased sympathetic nervous system activity and its therapeutic reduction in arterial hypertension, portal hypertension and heart failure. *J Auton Nerv Syst* **72**, 210–219.

Filosa JA, Bonev AD & Nelson MT (2004). Calcium dynamics in cortical astrocytes and arterioles during neurovascular coupling. *Circ Res* **95**, e73–81.

Fink GD (1997). Long-term sympatho-excitatory effect of angiotensin II: a mechanism of spontaneous and renovascular hypertension. *Clin Exp Pharmacol Physiol* **24**, 91–95.

Gao L, Wang W, Mann E, Finch M, Li Y, Liu D, Schultz HD & Zucker IH (2006). Sympathoexcitation in chronic heart failure: Ang II induced inhibition of voltage-gated $K^+$ channel, an in vivo and in vitro study. *FASEB J* **20**, A1202–A1203.

Gardiner SM & Bennett T (1986). Endogenous vasopressin and baroreflex mechanisms. *Brain Res* **396**, 317–334.

Geiger JR & Jonas P (2000). Dynamic control of presynaptic $Ca^{2+}$ inflow by fast-inactivating $K^+$ channels in hippocampal mossy fiber boutons. *Neuron* **28**, 927–939.

Goldberg JH, Tamas G & Yuste R (2003). $Ca^{2+}$ imaging of mouse neocortical interneurone dendrites: Ia-type $K^+$ channels control action potential backpropagation. *J Physiol* **551**, 49–65.

Gutkind JS, Kurihara M, Castren E & Saavedra JM (1988). Increased concentration of angiotensin II binding sites in selected brain areas of spontaneously hypertensive rats. *J Hypertens* **6**, 79–84.

Guyenet PG (2006). The sympathetic control of blood pressure. *Nat Rev Neurosci* **7**, 335–346.

Hamill OP, Marty A, Neher E, Sakmann B & Sigworth FJ (1981). Improved patch-clamp techniques for high-resolution current recording from cells and cell-free membrane patches. *Pflugers Arch* **391**, 85–100.

Hardy SG (2001). Hypothalamic projections to cardiovascular centers of the medulla. *Brain Res* **894**, 233–240.

Hartveit E & Veruki ML (2006). Studying properties of neurotransmitter receptors by non-stationary noise analysis of spontaneous synaptic currents. *J Physiol* **574**, 751–785.

Haywood JR, Mifflin SW, Craig T, Calderon A, Hensler JG & Hinojosa-Laborde C (2001). $\gamma$-Aminobutyric acid (GABA)-A function and binding in the paraventricular nucleus of the hypothalamus in chronic renal-wrap hypertension. *Hypertension* **37**, 614–618.

Herzig TC, Buchholz RA & Haywood JR (1991). Effects of paraventricular nucleus lesions on chronic renal hypertension. *Am J Physiol Heart Circ Physiol* **261**, H860–H867.

Hlubek MD & Cobbett P (2000). Differential effects of $K^+$ channel blockers on frequency-dependent action potential broadening in supraoptic neurons. *Brain Res Bull* **53**, 203–209.

Jackson MB, Konnerth A & Augustine GJ (1991). Action potential broadening and frequency-dependent facilitation of calcium signals in pituitary nerve terminals. *Proc Natl Acad Sci U S A* **88**, 380–384.

Judy WV, Watanabe AM, Henry DP, Besch HR Jr, Murphy WR & Hockel GM (1976). Sympathetic nerve activity: role in regulation of blood pressure in the spontaenously hypertensive rat. *Circ Res* **38**, 21–29.

Jung JY, Lee JU & Kim WJ (2004). Enhanced activity of central adrenergic neurons in two-kidney, one clip hypertension in Sprague-Dawley rats. *Neurosci Lett* **369**, 14–18.

Kang J, Huguenard JR & Prince DA (2000). Voltage-gated potassium channels activated during action potentials in layer V neocortical pyramidal neurons. *J Neurophysiol* **83**, 70–80.

Kannan H & Yamashita H (1983). Electrophysiological study of paraventricular nucleus neurons projecting to the dorsomedial medulla and their response to baroreceptor stimulation in rats. *Brain Res* **279**, 31–40.

Kasai H, Kameyama M, Yamaguchi K & Fukuda J (1986). Single transient K channels in mammalian sensory neurons. *Biophys J* **49**, 1243–1247.

© 2008 The Authors. Journal compilation © 2008 The Physiological Society

Katholi RE, Whitlow PL, Winternitz SR & Oparil S (1982). Importance of the renal nerves in established two-kidney, one clip Goldblatt hypertension. *Hypertension* **4**, 166–174.

Kim J, Wei DS & Hoffman DA (2005). Kv4 potassium channel subunits control action potential repolarization and frequency dependent broadening in hippocampal CA1 pyramidal neurons. *J Physiol* **569**, 41–57.

Kirkpatrick K & Bourque CW (1991). Dual role for calcium in the control of spike duration in rat supraoptic neuroendocrine cells. *Neurosci Lett* **133**, 271–274.

Kubo T, Hagiwara Y, Sekiya D, Chiba S & Fukumori R (2000). Cholinergic inputs to rostral ventrolateral medulla pressor neurons from hypothalamus. *Brain Res Bull* **53**, 275–282.

Lebrun CJ, Blume A, Herdegen T, Mollenhoff E & Unger T (1996). Complex activation of inducible transcription factors in the brain of normotensive and spontaneously hypertensive rats following central angiotensin II administration. *Regul Pept* **66**, 19–23.

Li J & Correa AM (2002). Kinetic modulation of HERG potassium channels by the volatile anesthetic halothane. *Anesthesiology* **97**, 921–930.

Li Z & Ferguson AV (1993). Angiotensin II responsiveness of rat paraventricular and subfornical organ neurons in vitro. *Neuroscience* **55**, 197–207.

Li Z & Ferguson AV (1996). Electrophysiological properties of paraventricular magnocellular neurons in rat brain slices: modulation of IA by angiotensin II. *Neuroscience* **71**, 133–145.

Li DP & Pan HL (2005). Angiotensin II attenuates synaptic GABA release and excites paraventricular-rostral ventrolateral medulla output neurons. *J Pharmacol Exp Ther* **313**, 1035–1045.

Li DP & Pan HL (2006). Plasticity of GABAergic control of hypothalamic presympathetic neurons in hypertension. *Am J Physiol Heart Circ Physiol* **290**, H1110–H1119.

Li DP & Pan HL (2007). Glutamatergic inputs in the hypothalamic paraventricular nucleus maintain sympathetic vasomotor tone in hypertension. *Hypertension* **49**, 916–925.

Li YF, Wang W, Mayhan WG & Patel KP (2006). Angiotensin-mediated increase in renal sympathetic nerve discharge within the PVN: role of nitric oxide. *Am J Physiol Regul Integr Comp Physiol* **290**, R1035–R1043.

Li Y, Zhang W & Stern JE (2003). Nitric oxide inhibits the firing activity of hypothalamic paraventricular neurons that innervate the medulla oblongata: role of GABA. *Neuroscience* **118**, 585–601.

Lindau M & Neher E (1988). Patch-clamp techniques for time-resolved capacitance measurements in single cells. *Pflugers Arch* **411**, 137–146.

Liu Y & Gutterman DD (2002). Oxidative stress and potassium channel function. *Clin Exp Pharmacol Physiol* **29**, 305–311.

Luther JA & Tasker JG (2000). Voltage-gated currents distinguish parvocellular from magnocellular neurones in the rat hypothalamic paraventricular nucleus. *J Physiol* **523**, 193–209.

Ma M & Koester J (1996). The role of $K^+$ currents in frequency-dependent spike broadening in *Aplysia* R20 neurons: a dynamic-clamp analysis. *J Neurosci* **16**, 4089–4101.

Magee J, Hoffman D, Colbert C & Johnston D (1998). Electrical and calcium signaling in dendrites of hippocampal pyramidal neurons. *Annu Rev Physiol* **60**, 327–346.

Magee JC & Johnston D (1997). A synaptically controlled, associative signal for Hebbian plasticity in hippocampal neurons. *Science* **275**, 209–213.

Martin DS & Haywood JR (1998). Reduced GABA inhibition of sympathetic function in renal-wrapped hypertensive rats. *Am J Physiol Regul Integr Comp Physiol* **275**, R1523–R1529.

Martinez-Maldonado M (1991). Pathophysiology of renovascular hypertension. *Hypertension* **17**, 707–719.

Moran O & Conti F (1990). Sodium ionic and gating currents in mammalian cells. *Eur Biophys J* **18**, 25–32.

Nagatomo T, Inenaga K & Yamashita H (1995). Transient outward current in adult rat supraoptic neurones with slice patch-clamp technique: inhibition by angiotensin II. *J Physiol* **485**, 87–96.

Nakata T, Takeda K, Itho H, Hirata M, Kawasaki S, Hayashi J, Oguro M, Sasaki S & Nakagawa M (1989). Paraventricular nucleus lesions attenuate the development of hypertension in DOCA/salt-treated rats. *Am J Hypertens* **2**, 625–630.

Oparil S, Sripairojthikoon W & Wyss JM (1987). The renal afferent nerves in the pathogenesis of hypertension. *Can J Physiol Pharmacol* **65**, 1548–1558.

Petty MA & Reid JL (1977). Changes in noradrenaline concentration in brain stem and hypothalamic nuclei during the development of renovascular hypertension. *Brain Res* **136**, 376–380.

Robertson WP & Schofield GG (1999). Primary and adaptive changes of A-type $K^+$ currents in sympathetic neurons from hypertensive rats. *Am J Physiol Regul Integr Comp Physiol* **276**, R1758–R1765.

Robinson HP, Sahara Y & Kawai N (1991). Nonstationary fluctuation analysis and direct resolution of single channel currents at postsynaptic sites. *Biophys J* **59**, 295–304.

Rogawski MA (1985). The A-current: how ubiquitous a feature of excitable cells is it? *Trends Neurosci* **8**, 214–219.

Rudy B (1988). Diversity and ubiquity of K channels. *Neuroscience* **25**, 729–749.

Sabatini BL & Regehr WG (1997). Control of neurotransmitter release by presynaptic waveform at the granule cell to Purkinje cell synapse. *J Neurosci* **17**, 3425–3435.

Serodio P & Rudy B (1998). Differential expression of Kv4 $K^+$ channel subunits mediating subthreshold transient $K^+$ (A-type) currents in rat brain. *J Neurophysiol* **79**, 1081–1091.

Shao LR, Halvorsrud R, Borg-Graham L & Storm JF (1999). The role of BK-type $Ca^{2+}$-dependent $K^+$ channels in spike broadening during repetitive firing in rat hippocampal pyramidal cells. *J Physiol* **521**, 135–146.

Sigworth FJ (1980). The variance of sodium current fluctuations at the node of Ranvier. *J Physiol* **307**, 97–129.

Sigworth FJ (1981). Covariance of nonstationary sodium current fluctuations at the node of Ranvier. *Biophys J* **34**, 111–133.

Smith PM & Ferguson AV (1996). Paraventricular nucleus efferents influence area postrema neurons. *Am J Physiol Regul Integr Comp Physiol* **270**, R342–R347.

Sonner PM & Stern JE (2007). Functional role of A-type potassium currents in rat presympathetic PVN neurones. *J Physiol* **582**, 1219–1238.

© 2008 The Authors. Journal compilation © 2008 The Physiological Society

Stern JE (2001). Electrophysiological and morphological properties of pre-autonomic neurones in the rat hypothalamic paraventricular nucleus. *J Physiol* **537**, 161–177.

Stewart AE & Foehring RC (2001). Effects of spike parameters and neuromodulators on action potential waveform-induced calcium entry into pyramidal neurons. *J Neurophysiol* **85**, 1412–1423.

Stocker SD, Simmons JR, Stornetta RL, Toney GM & Guyenet PG (2006). Water deprivation activates a glutamatergic projection from the hypothalamic paraventricular nucleus to the rostral ventrolateral medulla. *J Comp Neurol* **494**, 673–685.

Sumners C, Zhu M, Gelband CH & Posner P (1996). Angiotensin II type 1 receptor modulation of neuronal $K^+$ and $Ca^{2+}$ currents: intracellular mechanisms. *Am J Physiol Cell Physiol* **271**, C154–C163.

Sun C, Sellers KW, Sumners C & Raizada MK (2005). NAD(P)H oxidase inhibition attenuates neuronal chronotropic actions of angiotensin II. *Circ Res* **96**, 659–666.

Sundaram K, Johnson SM & Felder RB (1997). Altered expression of delayed excitation in medial NTS neurons of spontaneously hypertensive rats. *Neurosci Lett* **225**, 205–209.

Swanson LW & Kuypers HG (1980). The paraventricular nucleus of the hypothalamus: cytoarchitectonic subdivisions and organization of projections to the pituitary, dorsal vagal complex, and spinal cord as demonstrated by retrograde fluorescence double-labeling methods. *J Comp Neurol* **194**, 555–570.

Swanson LW & Sawchenko PE (1983). Hypothalamic integration: organization of the paraventricular and supraoptic nuclei. *Annu Rev Neurosci* **6**, 269–324.

Tagawa T & Dampney RA (1999). $AT_1$ receptors mediate excitatory inputs to rostral ventrolateral medulla pressor neurons from hypothalamus. *Hypertension* **34**, 1301–1307.

Takimoto K, Li D, Hershman KM, Li P, Jackson EK & Levitan ES (1997). Decreased expression of Kv4.2 and novel Kv4.3 $K^+$ channel subunit mRNAs in ventricles of renovascular hypertensive rats. *Circ Res* **81**, 533–539.

Traynelis SF, Silver RA & Cull-Candy SG (1993). Estimated conductance of glutamate receptor channels activated during EPSCs at the cerebellar mossy fiber-granule cell synapse. *Neuron* **11**, 279–289.

Villarroel A (1997). Nonstationary noise analysis of M currents simulated and recorded in PC12 cells. *J Neurophysiol* **77**, 2131–2138.

Wang D, Sumners C, Posner P & Gelband CH (1997). A-type $K^+$ current in neurons cultured from neonatal rat hypothalamus and brain stem: modulation by angiotensin II. *J Neurophysiol* **78**, 1021–1029.

Wheeler DB, Randall A & Tsien RW (1996). Changes in action potential duration alter reliance of excitatory synaptic transmission on multiple types of $Ca^{2+}$ channels in rat hippocampus. *J Neurosci* **16**, 2226–2237.

Yang Z, Bertram D & Coote JH (2001). The role of glutamate and vasopressin in the excitation of RVL neurones by paraventricular neurones. *Brain Res* **908**, 99–103.

Yang Z & Coote JH (1998). Influence of the hypothalamic paraventricular nucleus on cardiovascular neurones in the rostral ventrolateral medulla of the rat. *J Physiol* **513**, 521–530.

Yao JA & Tseng GN (1994). Modulation of 4-AP block of a mammalian A-type K channel clone by channel gating and membrane voltage. *Biophys J* **67**, 130–142.

Yoshimura Y, Kimura F & Tsumoto T (1999). Estimation of single channel conductance underlying synaptic transmission between pyramidal cells in the visual cortex. *Neuroscience* **88**, 347–352.

Zhang TT, Takimoto K, Stewart AF, Zhu C & Levitan ES (2001). Independent regulation of cardiac Kv4.3 potassium channel expression by angiotensin II and phenylephrine. *Circ Res* **88**, 476–482.

Zhou C, Ziegler C, Birder LA, Stewart AF & Levitan ES (2006). Angiotensin II and stretch activate NADPH oxidase to destabilize cardiac Kv4.3 channel mRNA. *Circ Res* **98**, 1040–1047.

Zhu GQ, Patel KP, Zucker IH & Wang W (2002). Microinjection of ANG II into paraventricular nucleus enhances cardiac sympathetic afferent reflex in rats. *Am J Physiol Heart Circ Physiol* **282**, H2039–H2045.

Zimmerman MC, Lazartigues E, Lang JA, Sinnayah P, Ahmad IM, Spitz DR & Davisson RL (2002). Superoxide mediates the actions of angiotensin II in the central nervous system. *Circ Res* **91**, 1038–1045.

Zimmerman MC, Sharma RV & Davisson RL (2005). Superoxide mediates angiotensin II-induced influx of extracellular calcium in neural cells. *Hypertension* **45**, 717–723.

## Acknowledgements

We thank Margaret Wood for her contribution to the morphometric studies. This work was supported by NIH RO1 HL68725 (J.E.S.).

© 2008 The Authors. Journal compilation © 2008 The Physiological Society